ЖУРНАЛ СТРУКТУРНОЙ ХИМИИ

2016. Том 57, № 8 *Ноябрь – декабрь* *С. 1649 – 1654*

UDC 541.6:548.737:541.65

STRUCTURAL CHARACTERIZATION, PHOTOPHYSICAL AND BSA BINDING INTERACTION STUDIES OF 4,4′-BIS(BENZIMIDAZOLYL)-2,2′-BIPYRIDINE

K. Swarnalatha[1], P. Rathnamala[1], A.A. Babu[1], N. Bhuvanesh[2]

[1]*Department of Chemistry, Manonmaniam Sundaranar University, Tirunelveli, Tamil Nadu, India*
E-mail: swarnalatha@msuniv.ac.in
[2]*Department of Chemistry and Biochemistry, University of Texas at Austin, Austin, USA*

Received September, 02, 2015 *Revised — December, 17, 2015*

The title compound is synthesized from the precursors 1,2-diaminobenzene and 2,2′-bipyridine-4,4′-dicarboxylic acid (dcbpy) and characterized using ESI-Mass, ^{1}H NMR, FT-IR and single crystal X-ray analysis. We are the first to report the crystal structure of the 4,4′-bis(benzimidazolyl)-2,2′-bipyridine (bimbpy) ligand. The photophysical properties of the compound in dimethyl sulfoxide and in the aqueous medium are studied. The interaction studies of bimbpy with bovine serum albumin (BSA) were performed with the fluorescence technique and it strongly binds with BSA.

DOI: 10.15372/JSC20160809

K e y w o r d s: 4,4′-bis(benzimidazolyl)-2,2′-bipyridine, crystal structure, energy transfer, BSA binding.

INTRODUCTION

Benzimidazoles are ″the privileged substructures″ for drug dosing due to their chemotheraupetic values. Benzimidazole containing molecules and their derivatives have been found in biologically active small molecules, such as vitamin B12 and also act as antitumor, antiparasitic, and antimicrobial agents [1]. The broad spectrum antibiotic nature of the benzimidazole moiety has appealed to researchers to synthesize many benzimidazole and polybenzimidazole type ligands. Because of their unique photophysical properties, these heterocyclic organic molecules have applications in drugs [2], synthetic fibers [3], organized assemblies [4], solar cell [5], proton exchange membranes in fuel cells [6], and also in the proton coupled electron transfer processes involved in many biological, catalytic, molecular, and photonic systems [7]. To understand the PCET process many ligands containing ionisable protons have been designed. Many such ligands containing the benzimidazole moiety have already been employed and their transition metal complexes were studied [8]. We have designed a new 4,4′-bis(benzimidazolyl)-2,2′-bipyridine ligand which contains two benzimidazole groups tied through the bipyridine moiety. The analogous ligands such as 2,2′-bis(benzimidazolyl)-4,4′-bipyridine, 6,6′-bis(benzimidazolyl)-2,2′-bipyridine and their transition metal complexes were already reported [9].

Serum albumins are the most abundant protein in plasma. They are responsible for the maintenance of blood pH and contribute to colloid osmotic pressure. Because of its homologous nature with human serum albumin, low cost, ease availability and ligand binding properties, BSA was selected as the protein model. Many research articles reported the interaction of BSA with drugs and dyes [10—13]. In this paper, a new 4,4′-bis(benzimidazolyl)-2,2′-bipyridine ligand was synthesized and charac-

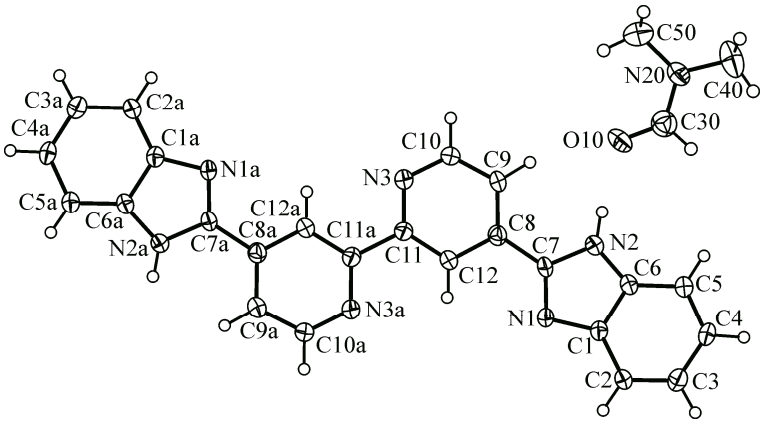

Fig. 1. ORTEP view of bimbpy

terized by IR, NMR, UV, single crystal XRD and the binding nature as well as the quenching mechanism between BSA and bimbpy were reported in detail using the luminescence technique.

EXPERIMENTAL

Materials. Reagent grade chemicals were used without further purification. 1,2-diaminobenzene (Merck) and 2,2′-bipyridine-4,4′-dicarboxylic acid (Alfa aesar) were used as received. Bovine serum albumin was obtained from Merck. Interaction studies were carried out in a Tris-HCl buffer solution (pH = 7.4) at 298 K. Solvents used were of spectroscopic grade.

Methods and instrumentation. Electronic absorption spectra were recorded on a Perkin Elmer Lambda 25 UV-Vis spectrometer. A JASCO FT-IR 410 spectrometer was used to record the IR spectra in the range 4000—400 cm^{-1} using KBr pellets. Emission intensity measurements were carried out using an Elico SL174 spectrofluorometer. The ^1H NMR spectrum was recorded on a Bruker-400 MHz NMR spectrometer. The electron spray mass spectrum was measured with a THERMO Finnigan LCQ Advantage max ion trap mass spectrometer.

X-ray crystallography. The crystals of the title compound of a suitable size were selected from the mother liquor and then mounted on the tip of a nylon loop. Intensity data for the crystal were collected using a Cu sealed X-ray tube (K_α = 1.5418 Å) fitted with a graphite monochromator on a BRUKER GADDS X-ray (three-circle) diffractometer. Integrated intensity information for each reflection was obtained by the reduction of data frames with APEX2 [14]. TWINABS [15] was employed to correct the data for absorption effects. The structures were solved by direct methods using SHELXS [16] and refined (weighted least squares refinement on F^2) to convergence. Platon [17] was used to verify the absence of additional symmetry and voids. Hydrogen atoms were placed in idealized positions and refined using the riding model. All non-hydrogen atoms were refined with anisotropic thermal parameters. In the crystallographic asymmetric unit cell, a ligand with two DMF molecules is present. The ORTEP view of the ligand structure along with the atom numbering scheme is shown in Fig. 1.

Preparation of the 4,4′-bis(benzimidazolyl)-2,2′-bipyridine (bimbpy) ligand. A mixture of *o*-phenylenediamine (1.108 g, 10 mmol), 2,2′-bipyridine-4,4′-dicarboxylic acid (1 g, 40 mmol) in syrupy *o*-phosphoric acid (25 ml) was heated for 2 h at 250 °C. The blue viscous solution was cooled to room temperature and poured into ice with stirring. A blue-violet precipitate thus obtained was slowly neutralized with aqueous ammonia. The light pink solid was formed, filtered, and washed with water. Colourless blocks of crystals were obtained by slow evaporation of the compound from dimethyl formamide (DMF). The off-white solid was completely soluble in DMSO. Yield 1.2 g (75 %); mp > 300 °C.

RESULTS AND DISCUSSION

Synthesis and characterization. The title compound 4,4′-bis(benzimidazolyl)-2,2′-bipyridine (bimbpy) was synthesised by condensing *o*-phenylenediamine with 2,2′-bipyridine-4,4′-dicarboxylic

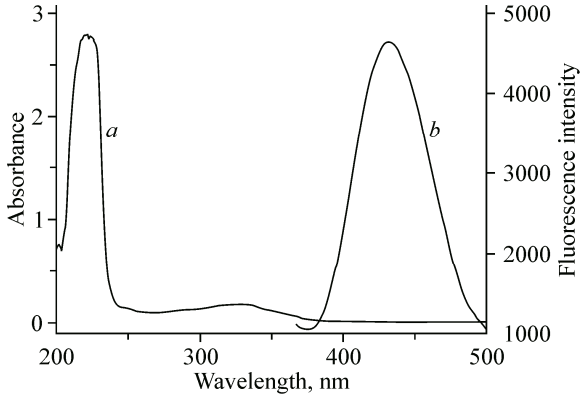

Fig. 2. Absorption (*a*) and emission spectrum (*b*) of bimbpy (1.0×10^{-5} mol·L^{-1}) in the Tris-HCl buffer at pH = 7.4, λ_{ex} = 326 nm

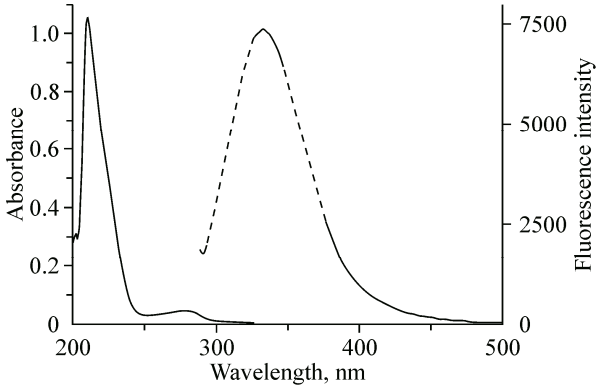

Fig. 3. Absorption (solid line) and emission spectrum (dotted line) of BSA (1.0×10^{-5} mol·L^{-1}) in the Tris-HCl buffer at pH = 7.4, λ_{ex} = 278 nm

acid and the colourless crystals were obtained from its DMF solution. The structure was confirmed from single crystal XRD. The crystal of the title compound belongs to the triclinic space group *P*-1, $a = 6.3593(3)$, $b = 10.9307(4)$, $c = 11.2875(4)$ Å, $\alpha = 65.761(2)°$, $\beta = 77.642(2)°$, $\gamma = 72.892(2)°$, $V = 679.86(5)$ Å^3, $Z = 1$, $D_{calc} = 1.306$ g/cm^3, $\mu = 0.693$ mm^{-1}, $F(000) = 282$, and final $R_1 = 0.0825$, $wR_2 = 0.2224$. The bond angles of the compound are as expected for this class of compound and the geometrical parameters are normal. The detailed crystallographic data and the selected bond distances and bond angles are available as CIF format (CCDC 994871).

The FT-IR spectrum showed the N—H peak at 3474 cm^{-1} and the peaks at 1665, 1600 cm^{-1} are due to benzimidazole and aromatic rings. The aromatic $\nu_{C—H}$ occurs at 1558, 1523, and 1434 cm^{-1}. The group of vibrations at 735 and 702 cm^{-1} are due to aromatic bending. The NMR spectrum shows 16 signals, it is a symmetric structure showing two downfield singlet at 13.54 δ corresponds to imidazole —NH protons. The signals appeared in the region 9.28 to 7.29 δ (14 protons) is assigned to benzimidazole and bipyridine protons. The ESI mass spectrum of the title compound shows a base peak at $m/z = 389$ (M = $C_{24}H_{16}N_6$).

Spectral studies. Absorption spectra of bimbpy has two peaks at 326 and 207 nm due to the imidazole centered π—π* transition and the bipyridine centered π—π* transition respectively. BSA has peaks at 210 and 278 nm in its electronic spectra. The peak at 278 nm was mainly due to tyrosine and tryptophan residues. The fluorescence spectrum of bimbpy displays a peak at 431 nm in the Tris-HCl buffer (pH = 7.4) (λ_{ex} = 326 nm). The protein, BSA emits at 332 nm in the Tris-HCl buffer (pH = 7.4) (λ_{ex} = 278 nm) (Figs. 2, 3).

Binding studies with BSA. Electronic spectra. The absorption spectrum of BSA was monitored in the presence of an increasing concentration of bimbpy (Fig. 4). The intensity of the 278 nm peak increases with an increase in the bimbpy concentration. Also during the reverse titration, i.e. the monitoring of the bimbpy spectrum in the presence of higher concentrations of BSA ended up in an increase in absorbance of the 320 nm peak. This evidences that the bimbpy/BSA ground state complex was formed.

Fluorescence quenching experiments. In order to find the binding mechanism, the binding site and the donor-acceptor distance, fluorescence titrations were carried out [18]. Fluorescence spectra of BSA in the presence of increasing bimbpy concentrations are shown in Fig. 5. With the addition of bimbpy, the fluorescence intensity of BSA was quenched and also the emission maximum gradually showed a red shift which indicated the less hydrophobic environment of the fluorophore. To find the quenching mechanism, Stern—Volmer quenching equation is used:

$$F_0/F = 1 + k_q\tau[Q] = 1 + K_{SV}[Q], \quad (1)$$

where F_0 and F correspond to the fluorescence intensity in the absence and presence of the quencher respectively, k_q is the quenching rate constant, τ is the BSA lifetime (10^{-8} s) in the absence of the quencher, K_{SV} is the Stern—Volmer quenching constant, and [Q] is the quencher concentration.

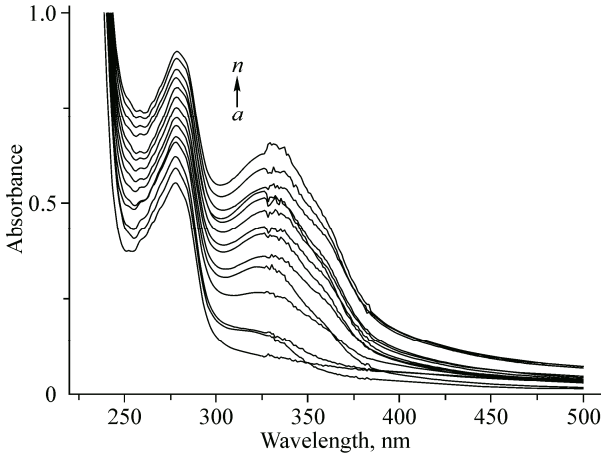

Fig. 4. Electronic ground state absorbtion spectral changes in BSA (1×10^{-5} mol·L^{-1}) with an incremental addition of bimbpy concentrations: 0 (*a*), 0.24 (*b*), 0.5 (*c*), 0.6 (*d*), 1.0 (*e*), 1.2 (*f*) ,1.4 (*g*), 1.44 (*h*), 1.5 (*i*), 1.6 (*j*), 1.66 (*k*), 1.7 (*l*), 1.74 (*m*), 1.8 (*n*) ($\times10^{-5}$ mol·L^{-1})

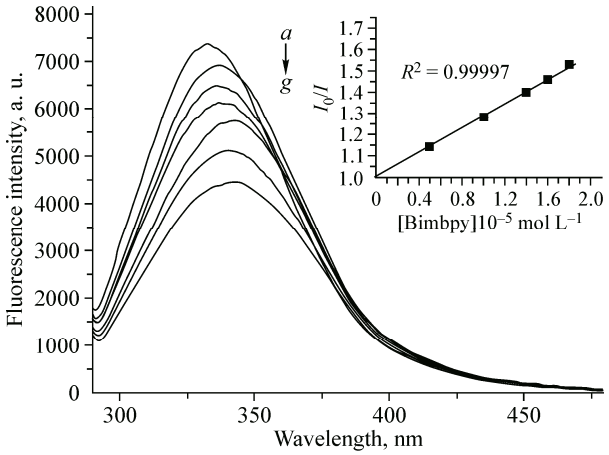

Fig. 5. Change in the emission intensity of BSA on incremental addition of bimbpy (*a*). (*a*—*g*) 0, 0.7, 0.8, 0.98, 1.0, 1.4, 1.6 ($\times10^{-5}$ mol·L^{-1}) (excited at 278 nm). The inset is the Stern—Volmer plot of BSA quenching by bimbpy. [BSA] = 1×10^{-5} mol·L^{-1} [bimbpy] ranges from 0.0 to 1.8×10^{-5} mol·L^{-1}

According to the literature [19], for dynamic quenching, the maximum collision quenching constant of various biopolymers is 10^{10} Mol^{-1}s^{-1}. The Stern—Volmer plot of the quenching of BSA fluorescence by bimbpy shows that within the investigated concentrations, the results agree with Stern—Volmer equation (1). From the plot, the K_{SV} and k_q ($= K_{SV}/\tau$) values were calculated. The Stern—Volmer quenching constant K_{SV} and the quenching rate constant k_q were found to be 2.92×10^4 L mol^{-1} ($r = 0.999$, SD = 0.006) and 2.92×10^{13} L mol^{-1}s^{-1} respectively. The rate constant of the protein quenching procedure initiated by bimbpy is greater than k_q of the scatter procedure. This means that the quenching is initiated by the formation of a complex, i.e. by static means, rather than by dynamic collision.

Binding constant and binding site. For the static quenching interactions, if it is assumed that there are similar and independent binding sites in the biomolecules, the relationship between the fluorescence intensity and the quenching medium can be deduced from the following formula:

$$M + nQ \rightarrow MQ_n, \quad (2)$$

where Q is the quencher, M is the biomolecule, and MQ_n is the quenched biomolecule whose resultant constant is K_a. Here,

$$K_a = [Q_n + M] / [Q]^n[B]. \quad (3)$$

If the overall amount of biomolecules (bound or unbound with the quencher) is M_0, then $[M_0] = [Q_n + M] + [M]$, here [M] is the concentration of unbound biomolecules, then the relationship between the fluorescence intensity and the unbound biomolecule as $[M] / [M_0] = F/F_0$ is

$$\log(F_0 - F)/F = \log K_b + n\log[Q], \quad (4)$$

where K_b is the binding constant and n is the number of binding sites. By plotting $\log(F_0 - F)/F$ against log[Q], K_b and n values were obtained from intercept and slope respectively. From Fig. 6, the K_b binding constant was found to be 4.196×10^4 L mol^{-1} and the n value was 1.033 at 298 K. The n value of approximately 1 indicates the existence of a single binding site in BSA for bimbpy.

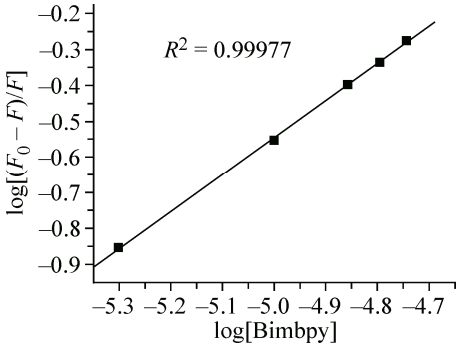

Fig. 6. Plot of $\log[(F_0 - F)/F]$ versus log[bimbpy]. [BSA] = $1\times$ $\times10^{-5}$ mol·L^{-1}. [bimbpy] ranges from 0.0 to 1.8×10^{-5} mol·L^{-1}

Energy transfer to bimbpy from BSA. Bimbpy can quench the intrinsic fluorescence of BSA remarkably through binding, which suggests the occurrence of energy transfer between the fluorophore in BSA and bimbpy. According to the Forster nonradiative energy transfer theory [20], the energy transfer rate depends on: (1) the relative orientation of the donor and acceptor dipoles; (2) the extent of overlap of the fluorescence emission spectrum of the donor with the absorption spectrum of the acceptor; and (3) the distance between the donor and the acceptor. The efficiency of energy transfer between the donor and the acceptor (E) is given by the following equation:

$$E = 1 - (F/F_0) = R_0^6/(R_0^6 + r^6), \quad (5)$$

where r is the distance between the protein residue and the bound ligand and R_0 is the critical distance when the energy transfer efficiency is 50 %. The R_0 value can be calculated using eqation

$$R_0^6 = 8.8\times10^{-25}K^2N^{-4}\varphi J, \quad (6)$$

where K^2 is the spatial orientation factor related to the geometry of the dipole donor-acceptor, $K^2 = 2/3$ for random orientation as in a fluid solution, N is the averaged refractive index of the medium in the wavelength range where the spectral overlap is significant, φ is the quantum yield of the donor, and J is the overlap integral between the fluorescence spectrum of the donor and the absorption spectrum of the acceptor. The J value can be calculated by the following equation:

$$J(\lambda) = \int_0^\infty F(\lambda)\varepsilon(\lambda)\lambda^4 d\lambda \,/\, F(\lambda)d\lambda, \quad (7)$$

where $F(\lambda)$ is the corrected fluorescence intensity of the donor at a wavelength λ with the total intensity normalized to unity and $\varepsilon(\lambda)$ is the molar extinction coefficient of bimbpy at a wavelength λ. The Forster distance (R_0) has been calculated assuming the random orientation of the donor and acceptor molecules. Here, $K^2 = 2/3$, $n = 1.366$, $\varphi = 0.51$ and from the available data it results that the overlap integral $[J(\lambda)] = 2.68$ cm^3 L mol^{-1}, the energy transfer efficiency (E) = 0.218, the critical energy transfer distance $R_0 = 0.95$ nm and the donor-acceptor distance $r = 1.18$ nm. The donor-to-acceptor distance is less than 8 nm, which indicates that the energy could transfer from BSA to bimbpy with a high probability and the distance is obtained by FRET with higher accuracy.

Conformational investigation. Synchronous fluorescence spectroscopy has been used to characterize complex mixtures which can provide fingerprints of complex samples. It involves the simultaneous scanning of excitation and emission monochromators. Synchronous fluorescence spectra give the information about the molecular environment around the chromophore and it is a useful method to determine the environment around aminoacids. When $\Delta\lambda$, the difference between the excitation and emission wavelengths, is stabilised at 15 or 60 nm, the spectral characteristics of protein tyrosine or tryptophan residues were observed respectively [21]. The effect of bimbpy on the synchronous fluorescence spectrum of BSA is shown in Fig. 7. When $\Delta\lambda = 15$ nm, the spectral maximum decreased and

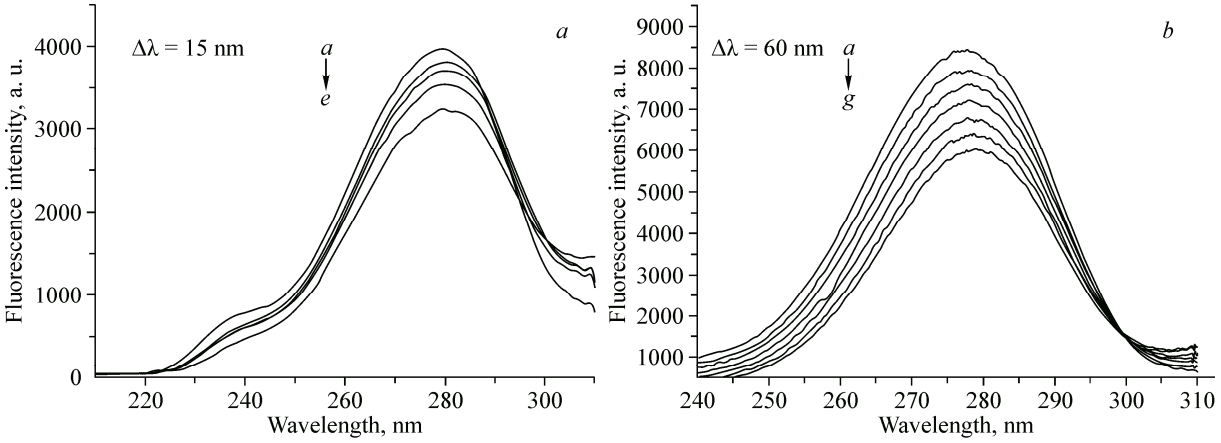

Fig. 7. Synchronous fluorescence spectra of BSA in the presence of bimbpy (*a*) $\Delta\lambda = 15$ nm and (*b*) $\Delta\lambda = 60$ nm. ($T = 298$ K, pH = 7.4). [BSA] = 1×10^{-5} mol·L^{-1} [bimbpy], (*a*—*e*) 0.6, 1.0, 1.4, 1.6, 2.0 ($\times10^{-5}$ mol·L^{-1})

shifted to a longer wavelength region. When $\Delta\lambda = 60$ nm, the intensity of the spectral maximum changed remarkably and shifted to the red end of the spectrum. This indicates that tryptophan and tyrosine experience a more polar environment in the presence of bimbpy. Due to its interaction with bimbpy, the BSA conformation changed and the polarity around the flurophores increased. Since the shift in the spectral maximum was more prominent during the $\Delta\lambda = 60$ nm scan, bimbpy lies closer to the tryptophan residue than to the tyrosine one. Also, the fluorescence quenching of BSA by bimbpy occurred due to the interaction of bimbpy with tryptophan residues present in BSA.

CONCLUSIONS

In this paper, we have designed, synthesised, characterized, and reported the crystal structure of a new 4,4′-bis(benzimidazolyl)-2,2′-bipyridine (bimbpy) ligand. The investigation of the interaction of BSA with bimbpy was made by absorption and fluorescence spectroscopy. Fluorescence experimental results showed that the quenching of BSA by bimbpy was due to the formation of the BSA—bimbpy complex following the static quenching and the non-radiative energy transfer was confirmed. As evident from the synchronous fluorescence spectrum, the conformations of both tyrosine and tryptophan residues changed and their microenvironment became more hydrophilic than it was in the presence of bimbpy.

This work was supported by the Department of Science and Technology (DST) and P. Rathnamala gratefully acknowledges University Grants Commission (UGC), New Delhi for the financial support through CSIR-UGC/JRF.

The X-ray crystallographic file in CIF format for the title compound is CCDC 994871.

REFERENCES

1. *Noolvi M., Agrawal S., Patel H., Badiger A., Gaba M., Zambre A.* // Arabian J. Chem. – 2014. – 7, N 2. – P. 219 – 226.
2. *Manisha S.K., Nachiket S.D., Shashikant R.P., Deepak S.M., Dipak T., Mayur B., Vinayak M.G.* // Pharma Chem. – 2010. – **2**, N 2. – P. 249 – 256.
3. *Vogel H., Marvel C.S.* // J. Polym. Sci. – 1961. – **50**, N 154. – P. 511 – 539.
4. *Hashimoto Y., Inoue M., Shindo H., Haga M.* // J. Inst. Sci. Eng. – 2001. – **7**. – P. 29 – 36.
5. *Huang W.K., Wu H.P., Lin P.L., Diau E.W.G.* // J. Phys. Chem. C. – 2013. – **117**, N 5. – P. 2059 – 2065.
6. *Yang J., Aili D., Li Q., Xu Y., Liu P., Che Q., Jensen J.O., Bjerrum N.J., He R.* // Polym. Chem. – 2013. – **4**, N 17. – P. 4768 – 4775.
7. *Weinberg D.R., Gagliardi C.J., Hull J.F., Murphy C.F., Kent C.A., Westlake B.C., Paul A., Ess D.H., McCafferty D.G., Meyer T.J.* // Chem. Rev. – 2012. – **112**, N 7. – P. 4016 – 4093.
8. (a) *Saha D., Das S., Bhaumik C., Dutt S., Baitalik S.* // Inorg. Chem. – 2010. – **49**, N 5. – P. 2334 – 2348. (b) *Yu S.C., Hou S., Chan W.K.* // Macromolecules. – 1999. – **32**, N 16. – P. 5251 – 5256.
9. (a) *Haga M., Ali M.M., Koseki S., Fujimoto K., Yoshimura A., Nozaki K., Ohno T., Nakajima K., Stufkens D.J.* // Inorg. Chem. – 1996. – **35**, N 11. – P. 3335 – 3347. (b) *Dutt S., Baitalik S., Ghosh M., Florke U., Nag K.* // Inorg. Chim. Acta. – 2011. – **372**, N 1. – P. 227 – 236. (c) *Ji B.M., Miao S.B., Deng D.S., Du C.X.* // Polyhedron. – 2009. – **28**, N 13. – P. 2611 – 2618.
10. *Shahabadi N., Hadidi S.* // Spectrochim. Acta, Part A. – 2014. – **122**. – P. 100 – 106.
11. *Xu H., Gao S.L., Lu J.B., Liu Q.W., Zuo Y., Wang X.* // J. Mol. Struct. – 2009. – **919**, N 1-3. – P. 334 – 338.
12. *Vlasova I.M., Kuleshova A.A., Vlasov A.A., Saletsky A.M.* // J. Mol. Struct. – 2013. – **1051**. – P. 86 – 94.
13. *Wang C.X., Yan F.F., Zhang Y.X., Ye L.* // J. Photochem. Photobiol. A. – 2007. – **192**, N 1. – P. 23 – 28.
14. *APEX2* ″Program for Data Collection and Integration on Area Detectors.″ – Madison, WI, USA: Bruker AXS Inc.
15. *Sheldrick G.M.* TWINABS, version 2008/1. – Germany: University of Göttingen, 2008.
16. *Sheldrick G.M.* // Acta. Crystallogr. A. – 2008. – **A64**. – P. 112 – 122.
17. *Spek A.L.* // J. Appl. Crystallogr. – 2003. – **36**. – P. 7 – 13.
18. *Sambrook J., Fritsch E.F., Maniatis T.* Molecular Cloning: A Laboratory Manual. – New York, Cold Spring Harbor Laboratory, 1989.
19. *Jiang C.Q., Gao M.X., He J.X.* // Anal. Chim. Acta. – 2002. – **452**, N 2. – P. 185 – 189.
20. *Modern* Quantum Chemistry / Eds. T. Forster, O. Sinnanoglu – New York : Academic Press, 1996.
21. *Miller J.N.* // Anal. Proc. – 1979. – **16**. – P. 203.